Transverse Stress Measured by Four-Polarization-State Frequency Domain Interferometry at High-Spatial Resolution*

R. Joseph Espejo and Shellee D. Dyer
National Institute of Standards and Technology
325 Broadway, Boulder, CO 80305 USA
Author email address: espejo@boulder.nist.gov

Abstract: We demonstrate a new method for measuring transverse stress with 11.8 μm spatial resolution in a fiber Bragg grating sensor, without the use of polarization maintaining fiber, by combining a four-state polarization analysis with a layer-peeling algorithm. Measurements of the externally induced birefringence agree well with predicted values.

Keywords: fiber Bragg gratings; fiber optic sensors; layer peeling; optical frequency-domain interferometry; transverse strain sensors.

1. Introduction

In this paper we present a simple fiber Bragg grating (FBG) strain sensor that yields high spatial resolution measurements of transverse stress. The sensor is interrogated with a frequency domain interferometer. The FBG is written in standard telecom single-mode fiber. Polarization information is obtained through a four-polarization-state analysis, so the system requires no polarization-maintaining fiber or components.

2.1 Model of transverse stress

When the FBG is transversely compressed, stress in the direction of the applied force, σ_y, is negative due to compression. Stresses in the two directions orthogonal to the applied force, σ_x and σ_z, are positive. When the region of uniform stress is longer than the diameter of the fiber, the stresses in the axial direction of the fiber, σ_z,, cancel, leaving only σ_x and σ_y. In this paper we limit ourselves to this case, so that axial elongations that would locally modify the grating's pitch are minimized.

The applied stress causes an anisotropic change in the refractive index, given by [1,2]

$$\begin{aligned} \delta n_x &= C_1\sigma_x + C_2\sigma_y \\ \delta n_y &= C_2\sigma_x + C_1\sigma_y; \\ C_1 &= -1.297\times10^{-6}\ {}^{mm^2}\!/_{N},\ C_2 = -4.835\times10^{-6}\ {}^{mm^2}\!/_{N}. \end{aligned} \tag{1}$$

The refractive index in the x- and y-directions is then given by $n_x = n_o+\delta n_x$ and $n_y = n_o+\delta n_y$, with birefringence

$$\Delta n = \delta n_y - \delta n_x. \tag{2}$$

The constants C_1 and C_2 are defined as the stress-optic coefficients for fused silica.

The actual refractive index structure of the FBG, specifically the FBG's effective index $n_{dc}(z)$, must then be measured for each birefringent eigenstate. This is accomplished through the application of an inverse scattering algorithm known as layer-peeling to the measured complex reflection spectrum of the FBG, as is described in [3], together with a four-state analysis, described below and in [4].

2.2 Four-state analysis

The four-state algorithm is a powerful yet simple tool for gathering polarization information from a system that does not have a polarization maintaining ability. The algorithm was originally developed for measuring polarization dependent loss (PDL) and polarization mode dispersion (PMD) in optical fibers and components and is also used to measure the polarization dependent wavelength shift (PDW) in FBGs [5-7]. In this paper we follow closely the method presented by [7], drawing on the relationship between PDW and the effective index.

In non-polarization maintaining fiber, a launched polarization state, ***S´***, will evolve into another arbitrary polarization state, ***S***, as it travels through the fiber to the FBG. However, in the absence of polarization-dependent loss and depolarization, several distinct launch states will maintain their orientation relative to one another on the Poincaré sphere, as is shown in Fig. 1. This is because all the states see the same birefringent effects in the fiber and thus undergo the same unitary transformation.

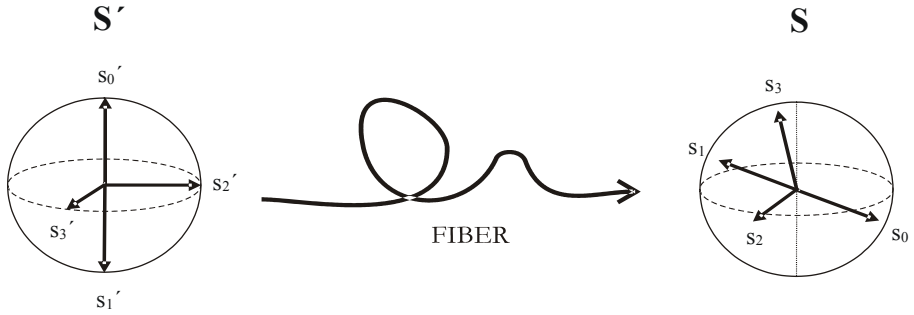

Figure 1. Schematic showing a length of fiber transforming the collection of states **S'** into arbitrary states **S**. The four launch states maintain their orientation with respect to each other as they propagate through the fiber.

To facilitate the four-state calculation we define a modified Poincaré sphere [4]. Plotted on the surface of this sphere is the local birefringence in the FBG, $\Delta n(z)$, is instead of power, as is usually done. The polarization coordinate axes remain the same. With this convention, the two orthogonal eigenaxes are mapped to the two linear states at the poles of the sphere. Each measurement of $n_{dc}(z)$ is the projection of the polarization vector at the grating on to the linear-state polar-axis of the Poincaré sphere.

Four states are needed to define the modified Poincare sphere, two of which are an orthogonal pair. The four states form a Mueller Set: three lie on a great circle on the sphere separated by 90° in Poincaré coordinates, and the fourth is on the axis of the great circle. For convenience we chose 0°, 90°, + 45°, and right-hand circular for the input states, $s_0´$, $s_1´$, $s_2´$, and $s_3´$.

To calculate Δn, which is the diameter of the modified Poincare sphere, we define equations (3)-(5). The equatorial value of the refractive index is given by

$$\overline{n} = \frac{n_{s0} + n_{s1}}{2}, \tag{3}$$

where n_{s0} and n_{s1} are the measured refractive indices of the orthogonal pair of states s_0, s_1. The value of $\overline{n}$ will always lie on the equator of the sphere, regardless of the orientation of the states s_0 and s_1, since s_0 and s_1 are an orthogonal pair. The direction cosine for each polarization state is given by

$$\delta n_{si} = \frac{\Delta n}{2}\cos\phi_{si} = n_{si} - \overline{n}; \quad i = 0,1,2,3\,. \tag{4}$$

The birefringence is then given by

$$\Delta n = 2\sqrt{\delta n_{s1}{}^2 + \delta n_{s2}{}^2 + \delta n_{s3}{}^2}\,. \tag{5}$$

The effective index n_{dc} values of the two eigenstates can then be expressed as $n_{dc}^{fast} = \overline{n} - \Delta n$ and $n_{dc}^{slow} = \overline{n} + \Delta n$.

3.1 Measurement system

The measurement system based on optical frequency-domain reflectometry (OFDR) is shown in Fig. 2. The measurement interferometer is a Fabry-Perot configuration, with the sensing FBG forming one end of the cavity and an air/glass interface of a butt-coupling inside a capillary being the other end. The gap of the butt-couple joint was carefully set to less than 5 μm. The distance between the butt-couple joint and the FBG is d = 18 cm, which forms a cavity with a free spectral range of 4.5 pm. For our sensing element we used a 1.5 cm long FBG with 11 dB peak reflectivity written in a common nonbirefringent single-mode fiber.

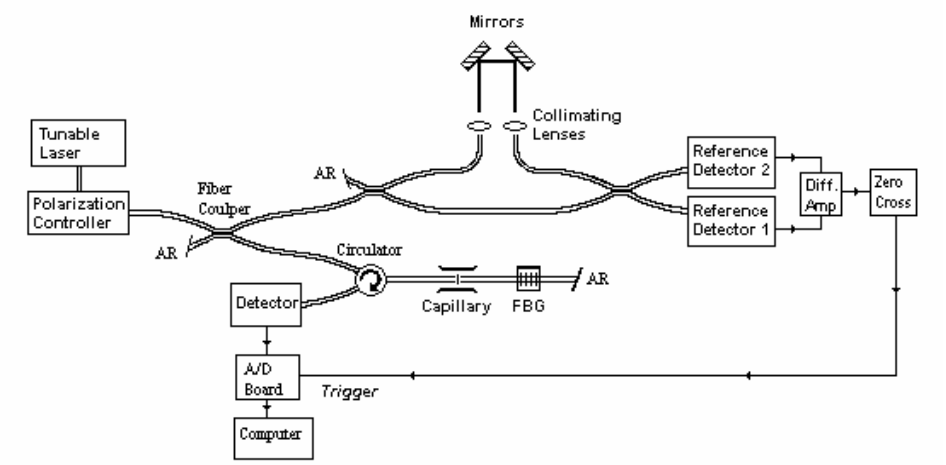

Figure 2. OFDR measurement system. Measurement interferometer is a Fabry-Perot configuration. An unbalanced Mach-Zender reference interferometer tracks the wavelength of the laser as it tunes, triggering the A/D sampling in order to compensate for nonlinear tuning. Polarization controller sets the tunable laser light to the desired polarization launch state.

Tuning non-linearity is corrected by an unbalanced Mach-Zender reference interferometer. The reference signal is differentially detected and used to trigger the A/D sampling at every zero crossing. The path imbalance used in the reference interferometer gives a sample spacing of about 0.5 pm, which over-samples the measurement Fabry-Perot interferometer signal 10 times per fringe. This signal is then digitized with a 16-bit A/D card.

A commercial fiber-coupled polarization controller is placed at the output of the tunable laser in order to set the desired polarization launch state. A measurement is then performed at each of the four polarization states. A simple layer-peeling algorithm is then used to calculate the complex spatial coupling coefficient of the FBG for each polarization state. From the coupling coefficient we can find the longitudinal refractive index of the FBG. The four-state analysis is then used to calculate the birefringence as a function of position along the fiber. The spatial resolution of the calculated FBG index profile is inversely related to the bandwidth of the laser's tuning range [3]. A spectral range from 1511 nm to 1580 nm gives a longitudinal spatial resolution for the FBG sensor of 11.8 μm.

3.2 Fiber loading fixture

Transverse loads are applied to the FBG with the fixture shown in Fig. 3. With this fixture a known compressive force can be applied to the FBG in a controlled manner by placing weights on top of the fixture. The test FBG and a support fiber are sandwiched between two thick polished glass plates. The support fiber ensures that the plates are parallel so that the compressive force is always perpendicular to the plates.

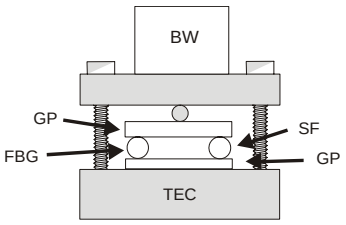

Figure 3. Schematic of the fiber loading fixture. SF: support fiber; GP: glass plate; BW: brass weight; TEC: thermal-electric cooler.

A metal pin is placed between the upper glass plate and the aluminum top plate, centered between the two fibers to prevent torsion of the load and to evenly distribute the load between the two fibers. In this configuration the force applied to the FBG is $mg/2$; m is the applied mass, and g is the gravitational constant. Two screws are used to hold the top plate in place and keep it from rotating out of position when the weights are added. The screws are left loose so as not to add any compression. The weights are balanced directly above the pin so that the screws affect the load as little as possible. The jacket was stripped from both the FBG and the support fibers. This is out of concern that permanent deformation of the soft jacket material caused by loading pressures might affect or influence later measurements in an unpredictable manner.

4. Results

A 660 μm wide aluminum strip was placed under the FBG in the loading fixture to produce a localized transverse stress. The FBG was measured with the OFDR system, and the birefringence, Δn, was found with the layer-peeling and four-state algorithms; the results are plotted in Fig. 4. Each measurement is the average of five sequential scans of the tunable laser.

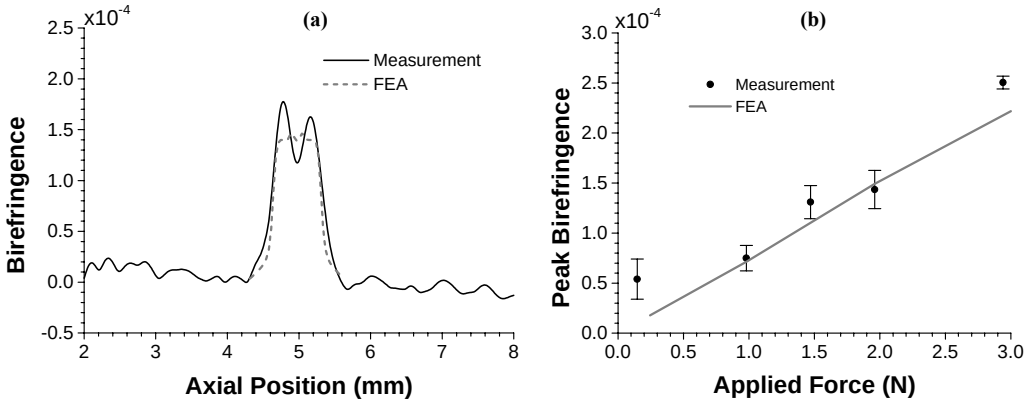

Figure 4: (a) Measured and calculated birefringence in the core of the FBG near the location of the localized strain created by the metal strip for a 2 N load. (b) The peak value of the birefringence in plot (a) as a function of applied force. for several different applied forces. Average and standard deviation (2σ) of four independent measurements. FEA: finite element analysis.

A finite element analysis model (FEA) was used to predict and verify the measured transverse stress in the FBG. The fiber was modeled as a solid cylinder of fused silica, 125 μm in diameter. The cylinder was then placed under a localized compressive load by a metallic block. The transverse stress values were computed along the axis of the cylinder, simulating the stress in the core of the FBG sensor. The FEA stress was calculated for a 660 μm wide block with the applied forces used in the measurement. There is good agreement between the measured birefringence and that predicted by FEA and equation (3). The measured birefringence profile in Fig. 4a matches the FEA profile reasonably well in overall width and height.

The cause for the peaks at the edges is most likely improper coupling between the aluminum strip and the FBG. It appears as though the fiber is bending around the strip, causing a higher stress at the edges and lower in the center. This non-uniform loading could explain the apparent noise in the measured peak birefringence in Fig. 4b.

6. Conclusion

We have demonstrated a fast and accurate transverse stress sensor with high spatial resolution. The flexibility and speed of the frequency domain interferometry technique used allows for a simplified sensor interrogation, compared to previous systems using time domain interferometric [4]. The fast measurement time allows for averaging to reduce noise. Additionally, this method has the potential for real time monitoring of the sensor, as well as being able to demultiplex a distributed sensor network. The high spatial resolution achieved by this method makes the sensor ideal for small-scale applications requiring high resolution, such as the testing of dental materials for microcracks and monitoring composite materials for internal delamination failures.

7. References

[1] C.M. Lawrence, D.V. Nelson, E. Udd and T. Bennett, "A fiber optic sensor for transverse strain measurement," *Exp. Mech.*, vol. 39, no. 3, pp. 202-209, 1999.

[2] R.B. Wagreich, E.A. Altia, H. Singh, and J.S. Sirkis "Effects of diametric load on fibre Bragg gratings in low birefringence fibre," *Elect. Lett.*, vol. 32, no. 13, pp. 1223-1224, 1996.

[3] J. Skaar, L. Wang, and T. Erdogan, "On the Synthesis of Fiber Bragg Gratings by Layer Peeling," *IEEE J. Quan. Elect.*, vol.37, no. 2, pp. 165-173, 2001.

[4] R.J. Espejo, S.D. Dyer, "High spatial resolution measurements of transverse stress in a fiber Bragg grating using four-state analysis low-coherence interferometry and layer-peeling," to be published in the proceeding of SPIE Smart Structures and Materials 2006, San Diego, CA.

[5] R.M. Craig, S.L. Gilbert, and P.D. Hale, "High-Resolution, Nonmechanical Approach to Polarization-Dependent Transmission Measurements," *J. Light. Tech.*, vol. 16, no. 7, 1998.

[6] P.A. Williams, "Modulation phase-shift measurement of PMD using only four launched polarisation states: a new algorithm," *Elect. Lett.*, vol. 35, no. 18, pp. 1578-1579, 1999.

[7] W.C. Swann, S.D. Dyer, R.M. Craig, "Four-state measurement method for polarization dependent wavelength shift," SOFM 2002, Boulder, CO, NIST Spec. Publ. 988, pp. 125-128, 2002.